10

Drought Analysis Based on SPI and SAD Curve for the Korean Peninsula Considering Climate Change

Minsoo Kyoung[1], Jaewon Kwak[2], Duckgil Kim[2], Hungsoo Kim[2] and Vijay P. Singh[3]
[1]*Samsung Loss Control Center, Samsung Fire & Marine Insurance. CO. Seoul*
[2]*Department of Civil Engineering, Inha University, Incheon*
[3]*Department of Biological and Agricultural Engineering Texas A & M University, College Station, TX 77843*
[1,2]*South Korea*
[3]*USA*

1. Introduction

In recent years, Korea has been experiencing serious drought and water scarcity problems. Korea is classified as a water-deficient country by the United Nations(UN). These problems are further compounded by the rapidly growing population, especially in the urban areas. Attaining water security is one of the major concerns and top priorities of the Korean government. Further complicating these issues is the global climate change, which is currently at the forefront of scientific research. With the projected global temperature increase due to increases in greenhouse gas emissions, scientists generally agree that the global hydrological cycle will intensify and suggest that extremes (e.g. droughts, floods) will become more common. Therefore, one major concern arising from climate change is its potential effects on water resources in terms of (increases in) droughts, and its impacts on different health, environmental, economic, and social sectors. Changes in the frequency and magnitude of droughts will have enormous impacts on water management, agriculture, and aquatic ecosystems. According to Korea Water Resource Association (KWRA), material damage recorded was 522 million USD in 1967, 584 million USD in 1968, 216 million USD in 1981, and 287 million USD in 1982 (http://kwra.or.kr/news/en_04.html). Researches on drought have, however, lagged behind in terms of quality and quantity.

This paper addresses the assessment of the drought characteristics in the Korean Peninsula considering climate change. Researches on temporal and spatial characteristics of drought are necessary to evaluate potential impact of drought and to carry out rational management of water resources. The most common method for interpreting drought relies on the drought index, which considers the impacts of drought severity, frequency, its affecting area, and duration. It is because the drought index explains the current drought situation by meteorological factors such as precipitation and past meteorological conditions close to that of the present.

Henriques and Santos (1999) proposed the use of thiessen method to produce SAF (Severity-Area-Frequency) curve. Hisdal and Tallaksen (2003), and Mishra and Singh (2009) also relied on SAF curve to analyze droughts. Furthermore, Kim et al. (2002) took advantage of geostatic technique used by Matheron (1963) to generate Intensity-Areal extent-Frequency curve. In one instance, SAD (Severity-Area-Duration) curves, in which the frequency in SAF curve is replaced by duration, were used to analyze the relationship between droughts and their areal extent (Andreadis et al., 2005). Precipitation data necessary for computing the SPI were obtained from a 32-years (1973-2004) dataset that originates from 58 stations operated by the Korea Meteorological Administration (KMA) and 130-years(1970~2099) dataset that was downscaled from GCM data to 58 stations of KMA. To produce SAD curves, it is necessary to expand SPI values for each of precipitation stations into the affected area. To do so, EOF analysis was carried out to contract data into core spatial information. Then, kriging method was used for spatial expansion. Climate change effect on drought was assessed by comparing SAD curves which were constructed from observed and downscaled precipitation respectively.

2. Climate change scenario for South Korea

2.1 Review of GCMs

Since the General Circulation Model (GCM) typically simulates the earth by putting a grid on it, peninsula states like Korea and some island countries tend to be depicted as part of sea, depending on location or the size of a grid. In this regard, reviewing whether Korea is described as land or not can allow this study to find an appropriate model for Korea. The reason is as follows: Since the GCM has disparate simulation models for land and sea, and once a land is presented as a sea in the simulation, consequent meteorological variables can present far distant results from reality. Figure 1 shows how GCMs differently suggested by countries describe the Korean peninsula.

As showed in Figure 1, the Korean Peninsula is simulated as a land in a few models, such as MIHR(Japan), CNCM3(France), and FGOALS(China) and other GCMs depict only some part of Korea as a land. In this study, therefore, such GCMs are excluded from reviews as they are assumed not suitable for the evaluation of climate change impacts on the Korean peninsula.

GCMs are known for their relatively precise simulation of temperatures. This study, thus, selected a CGM that properly presents the temperatures of the Koreans peninsula. The selection was done by comparing the grid-type temperature data of the central part of Korea, which is provided by the IPCC DDC, with the temperature data observed at Seoul weather station.

Among the simulation results from each GCM of 20c3m which simulates the 1990s, the statistics of monthly mean temperature (mean, variance, and distortion) of the center of the Korean peninsula was compared with that observed at Seoul station. Since 20c3m generally simulates the time period from 1985 to 1999, the statistics of monthly mean temperatures from 1961 to 1999 were firstly calculated and compared by taking into account the observation period. Several GCM models in Figure 1, such as MIHR, CNCM3, FGOALS which assume Korea as land, and other models, which describe some part of Korea as sea, were additionally reviewed for comparison as well.

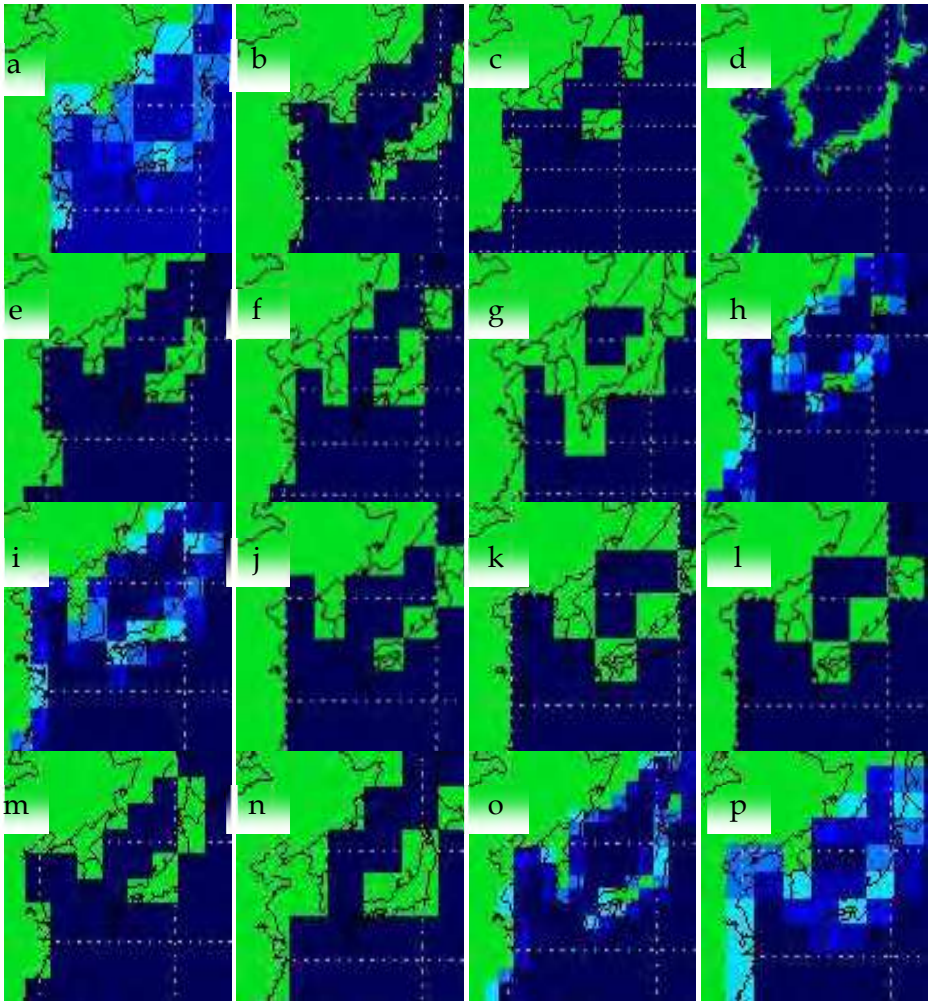

Fig. 1. GCMs grid around the Korea peninsular (a-BCM2, b-CGHR, c-CGMR, **d-MIHR**, e-CSMK3, **f-CNCM3**, **g-FGOALS**, h-CFCM20, i-CFCM21, j-GIAOM, k-GIEH, l-GIER, m-HADCM3, n-HADGEM, o-INCM3, p-IPCM4)

Overall, three models - MIHR, CNCM3, and FGOALS -, which assume Korea as land, simulate monthly mean temperatures of Korea relatively well. In the case of FGOALS, proposed meteorological variables have small variances. Thus, considering the nature of SK-NN method that detects and downscales the pattern of similar meteorological variables, it was expected that a number of locations would have several same precipitations. Therefore, this study had to eliminate FGOALS. Among CNCM3 and MIHR left, CNCM3, which was suggested as the most appropriate model for Korea in Kyoung (2010), was chosen, as the GCM for the analysis of drought on the Korean Peninsula.

	Jan	Feb	Mar	Apr	May	Jun	Jul	Aug	Sep	Oct	Nov	Dec
Seoul	-3.0	-0.7	5.0	11.6	18.0	21.0	25.6	25.5	20.8	14.3	6.8	-0.1
CNCM3	-3.3	-2.5	2.4	7.7	13.3	17.8	20.9	21.8	18.7	12.5	5.9	0.1
FGOALS	-7.0	-4.4	1.3	8.2	14.5	18.8	21.3	22.2	18.0	10.7	2.4	-4.0
MIHR	-3.3	-2.1	3.3	10.3	17.1	21.6	24.2	24.3	20.0	12.7	5.2	-0.4
GIAOM	18.0	18.6	20.0	22.0	24.2	25.8	26.4	26.3	25.0	23.0	20.7	19.5
GIEH	13.3	13.9	16.2	18.9	21.9	24.5	26.5	27.0	26.0	23.2	20.9	16.5
GIER	12.8	13.0	15.2	17.1	19.5	22.3	24.8	25.9	24.8	22.1	18.6	15.2
INCM3	4.4	5.8	10.3	15.5	20.8	24.8	26.8	26.8	24.5	19.3	12.8	6.6
IPCM4	14.9	14.2	15.6	18.5	21.9	24.9	26.7	27.1	26.1	23.6	20.6	17.4
MRCGCM	-1.6	-0.1	4.6	9.5	14.3	18.7	21.6	21.7	18.2	12.6	6.4	0.9

Table 1. Comparison of monthly mean temperature between observation and simulation from GCMs

	Jan	Feb	Mar	Apr	May	Jun	Jul	Aug	Sep	Oct	Nov	Dec
Seoul	5.1	3.6	2.4	1.7	0.8	0.7	1.6	1.2	0.7	1.2	2.3	3.5
CNCM3	5.2	3.5	2.4	1.0	1.3	1.4	0.7	0.7	0.8	0.7	1.1	1.3
FGOALS	4.9	5.7	4.4	1.6	0.5	0.5	0.3	0.3	0.6	1.9	3.2	4.5
MIHR	2.5	1.7	1.3	0.8	0.5	0.6	0.5	0.5	0.5	0.6	1.1	1.3
GIAOM	0.6	0.8	1.1	1.5	1.2	0.4	0.1	0.2	0.9	1.5	1.7	0.4
GIEH	1.9	1.9	1.5	0.6	0.5	0.5	0.2	0.2	0.4	0.5	1.0	1.4
GIER	1.7	1.9	0.8	0.4	0.3	0.4	0.3	0.3	0.5	0.9	1.2	0.7
INCM3	4.4	6.0	3.8	1.6	1.3	0.4	0.2	0.2	0.5	1.0	1.5	3.6
IPCM4	1.0	1.0	1.5	1.0	0.7	0.5	0.3	0.3	0.3	0.6	0.7	0.9
MRCGCM	1.5	1.1	1.1	0.8	0.4	0.3	0.4	0.7	0.7	1.0	1.5	1.0

Table 2. Comparison of variance of monthly mean temperature between observation and simulation from GCMs

	Jan	Feb	Mar	Apr	May	Jun	Jul	Aug	Sep	Oct	Nov	Dec
Seoul	-0.4	0.2	-0.6	0.9	0.2	0.0	0.7	-0.5	0.8	0.5	-0.1	-0.7
CNCM3	-2.2	-0.6	0.1	-0.6	-0.9	0.0	-1.4	0.1	0.4	-0.2	1.0	-0.1
FGOALS	-0.3	0.0	0.2	-0.4	0.0	-0.2	-0.6	-0.4	0.3	0.6	-0.5	-0.2
MIHR	-0.4	0.3	-0.8	0.1	0.3	-0.4	0.9	-0.5	0.5	0.3	0.7	-0.8
GIAOM	-0.4	-0.5	-0.2	0.0	-0.1	-0.3	-0.1	-0.5	-0.2	0.0	-0.2	-0.9
GIEH	-0.2	-0.1	-0.2	-0.4	-0.1	-0.1	0.2	0.1	0.2	0.2	-0.3	0.4
GIER	-0.3	0.4	-0.3	0.3	0.2	0.2	0.2	0.1	-0.2	-0.6	0.2	0.4
INCM3	0.2	-0.3	-0.2	-0.3	-0.1	-0.5	0.0	0.2	0.5	-0.4	0.0	-0.6
IPCM4	0.1	0.4	0.4	0.3	0.6	-0.2	-0.4	-0.9	-0.4	0.5	-0.2	-0.3
MRCGCM	-0.2	0.4	0.3	-0.3	-0.6	0.4	0.8	0.5	0.1	-0.1	-0.2	-0.1

Table 3. Comparison of skewness of monthly mean temperature between observation and simulation from GCMs

2.2 Application of downscaling technique

1) Selecting a climate change scenario

In this study, the SRES A1B scenario was selected as a socioeconomic scenario to predict the precipitation changes in Korea. This is because this study recognized the A1B scenario as the best match for circumstances under which the entire world is exerting great efforts to maximize the efficiency of energy resources and find alternative energy sources. And this study also examined how drought and probability precipitation in Korea can change, should the A1B scenario be considered on the basis of the 20c3m scenario used as the initial conditions of the SRES scenario.

In order to predict the impact of climate change on Korea in the short, medium, and long term, the time periods were divided as the followings:

CASE 1 (1980s) : 1970 ~ 1999 (20c3m, Reference duration)
CASE 2 (2020s) : 2010 ~ 2039 (A1B, Projection duration)
CASE 3 (2050s) : 2040 ~ 2069 (A1B, Projection duration)
CASE 4 (2080s) : 2070 ~ 2099 (A1B, Projection duration)

2) Adopting a spatial downscaling technique using the SK-NN method

A general K-NN technique is mainly used for short term prediction after estimating parameters($\widehat{\alpha_1}, \widehat{\alpha_2}, \ldots \ldots \widehat{\alpha_\alpha}$) necessary for prediction by considering delay time(τ) and embedding dimensions(m) in a single time series. This K-NN method, which was proposed by Casdagli (1992), and Casdaglli and Weigend (1994), is a method primarily applied to Chaos time-series under the assumption that past time-series patterns would be repeated in the future after converting the time series data of a single variable into a set of vectors with the consideration of its delay time and embedding dimension. This method was also used in studies of Young(1994), Lall and Sharma(1996), Lall et al.(1996), Rajagopalan and Lall(1999), Buishand and Brandsma(2001), Yates et al. (2003), Sharif and Burn(2006).

This study downscaled data from the meteorological variables provided monthly to monthly total precipitations observed by stations by applying the SK-NN (Simplest K-Nearest Neighbor) method, a simplest method of K-NN. This was based on the assumption that under the condition of specific hydrometeorological variables, the same precipitation can occur. Therefore, vectors were formed by using temperature, specific humidity, wind speed and sea level pressure which affect precipitation not using a single time series. Delay time was excluded, because it is insignificant, given that monthly mean by averaging original time series data is used. Embedding dimension was assumed to have four dimensions of meteorological variables – temperature, specific humidity, wind speed and sea level pressure – used in the downscale method.

Above all, for application, a set of vector needs to be constructed with meteorological variables of the NCEP data, including temperature, specific humidity, wind speed and sea level pressure, capable of affecting the precipitation which is intended to be downscaled, as follows:

$$Y_t = (a_t, b_t, c_t, \ldots\ldots, n_t)$$

Here, **n**is the number of meteorological variables affecting the variables to be downscaled, and **t** shows that the variables are time-series data, implying there **t** is number of vector Y_t. In addition, in order to calculate the optimal number of nearest (k), provided vector Y_t was

divided by Training set, Y_{ttra} and Prediction set, Y_{tpre}. In order to investigate the similarity between Y_{tpre} and Y_{ttra}, this study calculated the distance between them, or $\|Y_{tpre} - Y_{ttra}\|$. When the most similar Y_{ttra} with Y_{tpre} is identified through the process, the precipitation which occurred under the condition of Y_{ttra} is inferred to occur again in Y_{tpre}. Here, the number of nearest is determined by the number of which leads to a optimal result, while it is changing the number of similar Y_{ttra} with Y_{tpre} in order of its similarity. With the number of the nearest determined, Y_t is identified as many as the number of the nearest, then, precipitation at Y_t'.is calculated by getting arithmetic means of precipitation at Y_t,

This study selected appropriate meteorological variables like average temperature, humidity, southerly wind and sea level pressure for the downscale method, and downscaled precipitation data of 58 stations country-wide relevant to 20c3m and A1B scenarios from CNCM3 model.

This study initiated calibration and validation of the SK-NN model by using NCEP data and total precipitation data from stations in order for the application of SK-NN. To this end, the observed data was divided into three parts – Training set, Calibration set and Validation set. The first step for calibration is to find a duration that has the meteorological variable of NCEP value similar to the meteorological variables of NCEP – average temperature, humidity, southerly wind and sea level pressure – relevant to a calibration period. Then, the precipitation in locations is designated as the precipitation for the calibration period. In this case, the estimation of errors by increasing the number of meteorological variable groups of Training set from one to twenty, which are similar to the meteorological variables of NCEP relevant to calibration period, may produce K, the number of optimal meteorological variable groups for SN-NN. In order to evaluate the application of estimated value of K, the calibration was proceeded as follows: (See Figure 2)

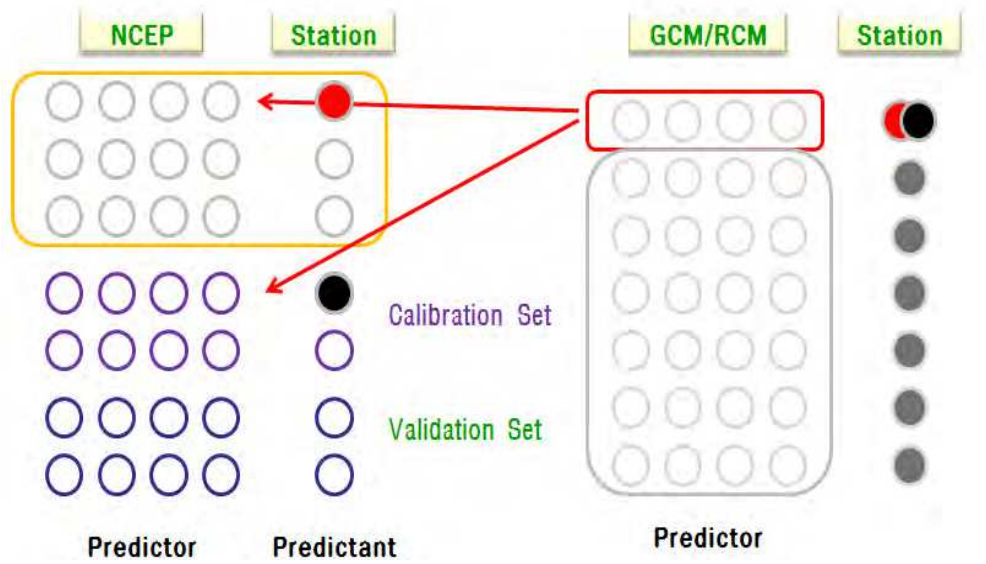

Fig. 2. Basic concept of Simplest K-NN method as a downscaling technique

When the application of the model is estimated through calibration and validation, it may be possible to get the precipitation of target locations of GCM by using the same meteorological variables with those of NCEP – average temperature, humidity, southerly wind and sea level pressure – suggested by GCM. In other words, the precipitation values for GCM may be estimated by averaging the results of extracted K number of meteorological variable groups of NCEP – average temperature, humidity, southerly wind and sea level – which have the same values with those of GCM.

3) Bias Correction by using Quantile Mapping

Those downscaled results from GCM tend to show some level of bias against observed outcomes in real. The most commonly used method to correct such bias is Quantile mapping suggested by Panofsy and Brire (1963). The Quantile mapping approach used as a way to correct runoff (Wood et al, 2004; Hamlet et al, 2003; Hashino et al., 2007), and in regard to climate change, GCM data in Palmer et al(2004), Fowler et all(2007b), Durman et al.(2001), Kim et al(2008), Kyoung et al(2009a, 2009b). The Quantile mapping's general procedure is presented in Figure 3.

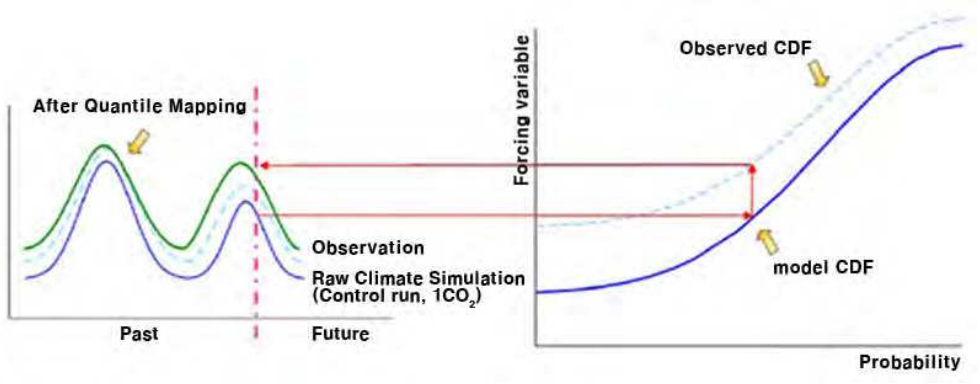

Fig. 3. Quantile mapping.

With the Quantile mapping approach, this study estimated the bias of observed data and GCM , with respect to both the monthly total precipitation of 20c3m(CASE1) scenario, which was downscaled by SK-NN, and that of 58 stations operated by the Korea Meteorological Administration (KMA). Then, the results were applied to those downscaled cases of A1B, CASE2, CASE3 and CASE4, to correct monthly total precipitation bias for each case.

4) KMA RCM

The National Institute of Meteorological Research (NIMR) in Korea is providing downscaled RCM for the Eastern Asia region. It uses the IPCC SRES A1B, A2 and B1, and generates a global climate change scenario by applying anthropogenic forcing to ESHO-G. It also generates a regionally downscaled climate change scenario for Korea by proceeding dynamical downscaling of a global climate change scenario with a regional climate model, MM5. Finally, it offers a high resolution climate change scenario by using a statistical downscaling technique.

3. Standardized precipitation index considering climate change

3.1 Standardized precipitation index

In this study, downscaled data for 58 stations were used to construct SPI for each of stations. SPI, which was developed by Mckee et al. (1993), is a relatively simple drought index based only on precipitation. Table 4 shows the status of droughts in accordance with the scope of index.

SPI	Moisture
more than 2.00	extremely wet
1.50 ~1.99	severe wet
1.00 ~ 1.49	wet
-0.99 ~ 0.99	normal
-1.49 ~ -1.00	dry
-1.99 ~ -1.50	severe dry
less than -2.00	extremely dry

Table 4. Classification of moisture by SPI

The SPI is calculated from the long term record of precipitation in each location (generally at least 30 years). Values of SPI are derived by comparing the total cumulative precipitation for a particular station or region over a specific time interval with the average cumulative precipitation for that same time interval over the entire length of the record. The SPI was

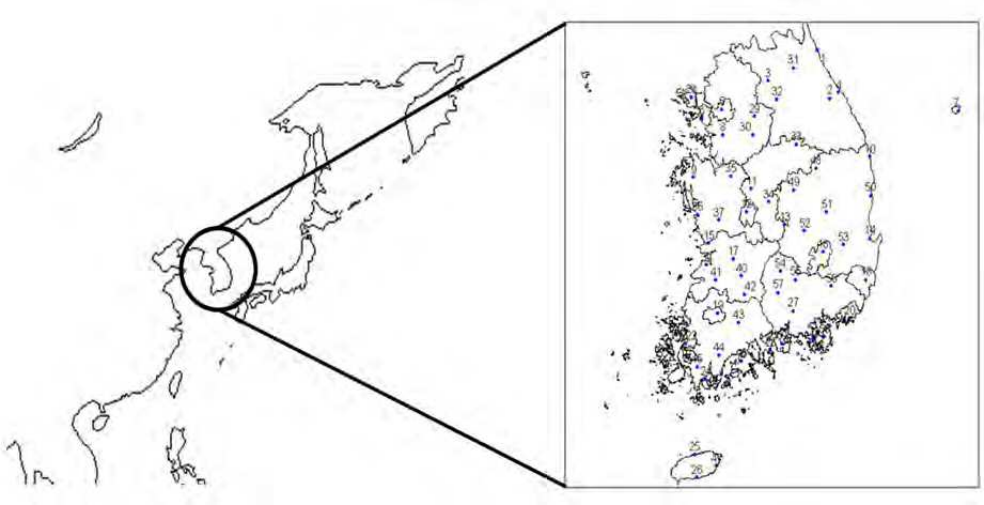

Fig. 4. Locations of Rainfall station, Korea

designed to enhance the detection of onset and monitoring of drought conditions on a variety of time scales. A key feature of the SPI is the flexibility to measure drought at different time scales. The data will be fitted to normal distribution and be normalized to a flexible multiple time scale such as 3-, 6-, 12-, 48-month and etc. This temporal flexibility allows the SPI to be useful in both short-term agricultural and long-term hydrological applications.
Figure 4 and Table 5 show the location and geographical designation of precipitation stations of Korea Meteorological Administration that provided data for the calculation of the SPI. Finally, Figure 5 ~ Figure 8 show the calculated SPI in conjunction with major locations.

No.	Station	No.	Station	No.	Station	No.	Station
1	Sokcho	16	Daegu	31	Inje		
2	Daegwallyong	17	Jeonju	32	Hongcheon	46	Sungsanpo
3	Chuncheon	18	Ulsan	33	Jecheon	47	Yeongju
4	Gangneung	19	Gwangju	34	Boeun	48	Mungyeong
5	Seoul	20	Pusan	35	Cheonan	49	Youngdong
6	In Cheon	21	Tongyeong	36	Boryeong	50	Uiseong
7	Ulleungdo	22	Mokpo	37	Buyeo	51	Gumi
8	Suwon	23	Yeosu	38	Buan	52	Yongcheon
9	Seosan	24	Wando	39	Imsil	53	Gochang
10	Uljin	25	Jeju	40	Jeongeup	54	Hapcheon
11	Chongju	26	Seogwipo	41	Namwon	55	Miryang
12	Daejeon	27	Jinju	42	Suncheon	56	Sancheong
13	Chupungryong	28	Ganghwa	43	Jangheung	57	Geoje
14	Pohang	29	Yangpyong	44	Haenam	58	Namhae
15	Gumsan	30	Icheon	45	Goheung		

Table 5. Rainfall stations

3.2 Assessment of climate change effect on drought occurrence and frequency

This study calculated SPI for precipitation at downscaled 58 stations in order to assess climate change effect on drought, and drought spell based on the estimated SPI. The drought spell may be assessed by SPI and using average precipitation index implies that SPI is constantly less than zero and its minimum value is less than -1(Dubrovsky et al, 2004). Building on droughts selected by such basis, climate change inducing a drought occurrence behavior was analyzed, and for this, droughts with the duration of 6 months and 12 months were selected.

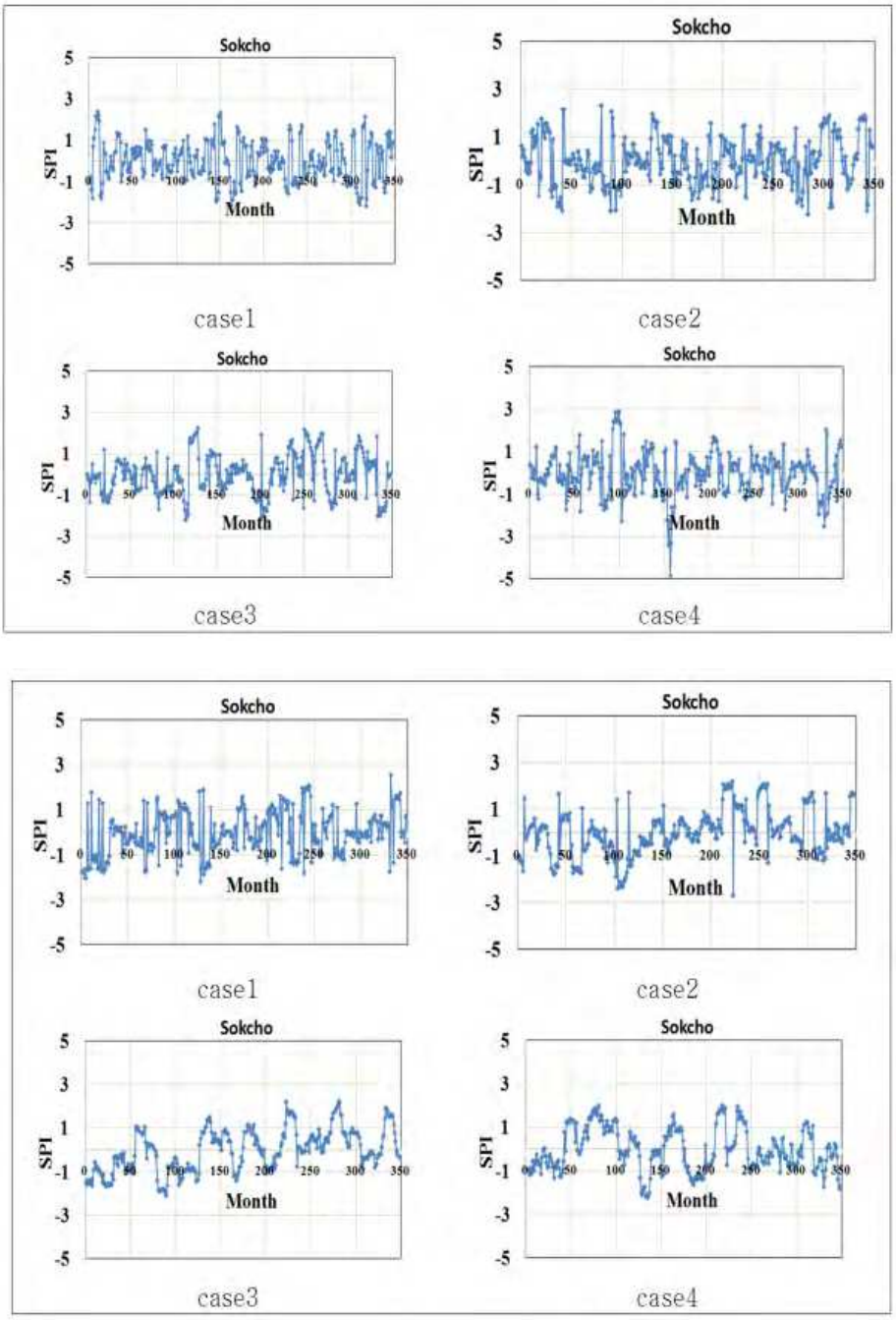

Fig. 5. SPI results of Sokcho (upper part: CNCM3 & downer part : KMA RCM)

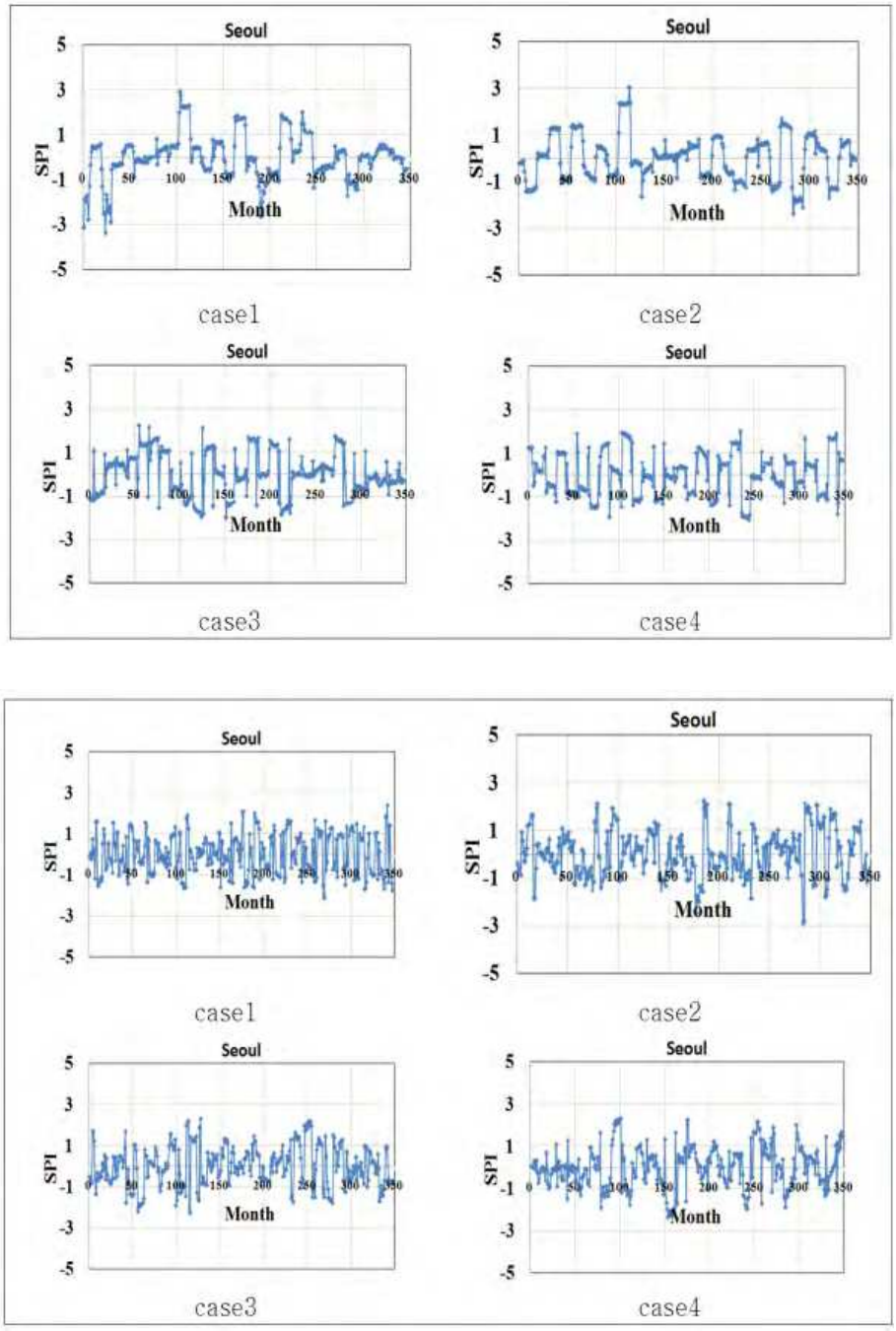

Fig. 6. SPI results of Seoul (upper part: CNCM3 & downer part : KMA RCM)

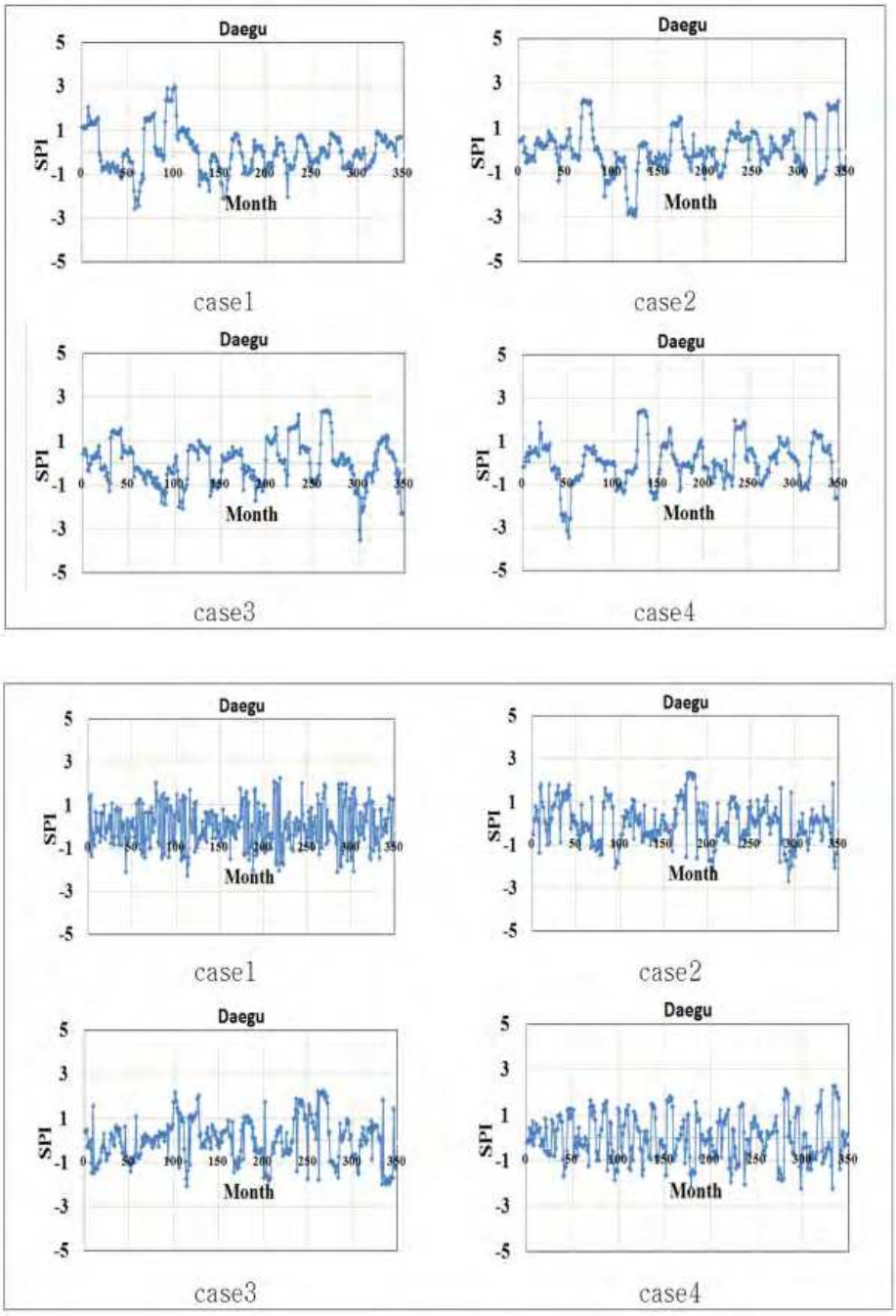

Fig. 7. SPI results of Daegu (upper part: CNCM3 & downer part : KMA RCM)

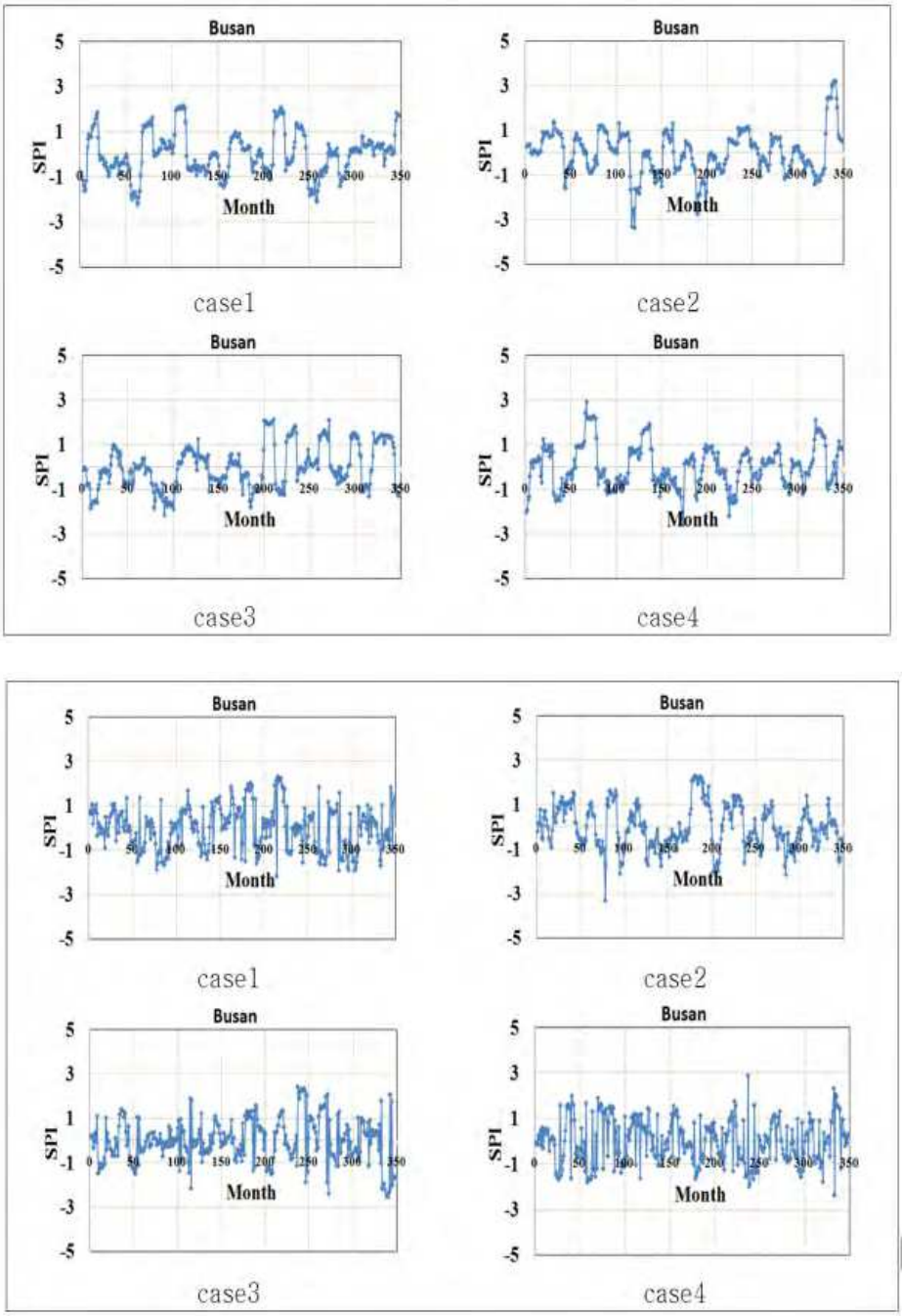

Fig. 8. SPI results of Busan (upper part: CNCM3 & downer part : KMA RCM)

GCM	Station	CASE1	CASE2	CASE3	CASE4	CASE1	CASE2	CASE3	CASE4
		more than 6 month				more than 12 month			
KMA RCM	Sokcho	1	2	5	3	0	0	0	0
	Seoul	2	2	2	4	0	0	0	0
	Daegu	0	4	4	2	0	0	0	0
	Busan	3	1	4	3	0	0	0	0
CNCM3	Sokcho	3	3	5	2	0	0	2	2
	Seoul	4	4	5	5	0	1	0	0
	Daegu	3	3	3	4	0	1	1	1
	Busan	4	3	2	2	1	2	1	0

Table 6. Frequencies of drought

Across those 58 stations, there are 138 droughts with the six-month duration in CASE1, 68 in CASE2, 171 in CASE3 and 121 in CASE4. In other words, the number of drought occurrences decreases in CASE2, and increases in CASE3, and then drops again. As for the CNCMs model, there are 185 droughts with the six-month duration in CASE1, 221 in CASE2, 190 in CASE3, and 186 in CASE4 across 58 stations, implying that the number of droughts is likely to increase in the future.

KMA RCM showed that there are five droughts with the 12-month duration in CASE1, zero in CASE2, seven in CASE3 and three in CASE$, representing that droughts with a longer duration may not return. Meanwhile, CNCM3 showed 50, 60, 38 and 35 times of drought for each case. It is possible to predict that the drought with the 12-month duration and above may steadily decrease due to the effect of climate change. This may be explained by the fact that the effect of gradually increasing precipitation reduces the number of drought occurrences with relatively a longer duration.

Table 7 shows the average severity of drought in major locations by drought duration (six and twelve months).

The average severity of the droughts with the duration of more than six months was -1.16, -0.95, -1.31, and -1.41 for each CASE in KMA RCM. For CASE4, as showed in Table 6, although the number of drought occurrences decreases, their severity increases, representing a possibility of much severe drought in the future. As for CASE2 of CNCM3, it was expected that relatively severe drought is likely to occur in the south central area, particularly Dae-gu, and some part of the southern coastal area. For CASE3 and CASE4, some parts of the southern coastal area and nearby inland areas were expected to be the main area affected by droughts though the potential drought areas may be reduced.

KMA RCM failed to simulate drought with the duration of over 12 months. So, when analyzing the average severity of such drought based on the CNCM3 model that successfully simulated the number of observed drought occurrences, it was predicted that droughts would occur mainly in the southern and eastern coastal area and Gangwon province. It was also predicted that such expected areas of drought would slightly decline through CASE3 and CASE4. In general, it can be predicted that drought with the duration of 12 months or more would slowly decrease because of climate change effects and this may be because drought with relatively a longer duration decreases as precipitation gradually increases.

4. Establishment of SAD curve

The empirical orthogonal function (EOF) is mainly used for indentifying major patterns of spatial variability. EOF analysis is widely applied to water resources management field

(Sauquet et al., 2000; Benjamin, 2002; Hisdal and Tallaksen, 2003; Yoo and Kim, 2004; Viron et al., 2006; Zveryaev and Arkhipkin, 2008; Perry and Niemann, 2008).

GCM	Station	CASE1	CASE2	CASE3	CASE4	CASE1	CASE2	CASE3	CASE4
		more than 6 month				more than 12 month			
KMA RCM	Sokcho	-1.7	-1.5	-1.6	-1.9	0	0	0	0
	Seoul	-1.4	-1.5	-1.8	-1.6	0	0	0	0
	Daegu	0.0	-1.6	-1.7	-1.7	0	0	0	0
	Busan	-1.4	-1.7	-1.6	-1.5	0	0	0	0
CNCM3	Sokcho	-1.5	-1.8	-1.5	-1.6	0.0	0.0	-1.61	-1.6
	Seoul	-1.4	-1.5	-1.4	-1.4	0.0	-1.8	0.0	0.0
	Daegu	-1.5	-1.9	-1.6	-1.7	0.0	-2.6	-1.9	-2.5
	Busan	-1.3	-1.6	-1.6	-1.4	-1.6	-1.9	-1.6	0.0

Table 7. Average severity for the occurred drought

In this study EOF analysis is applied to SPI in order to analyze quantitatively the regional behavior of drought. The individual EOFs are obtained by performing the SVD (single value decomposition) for the original data matrix A and the equation is as follows;

$$A = U \times S \times V^T$$

where columns of the matrix U are the EOFs of A, and each EOF is a mutually independent component. Diagonal components of the matrix S are the eigen values of A, and the sum of them is the variance of the original data. Each column of the matrix V is the coefficient of time series and represents the temporal behavior of the corresponding EOF. The matrix A is consisted of the number of locations (M) and the temporal length of SPI (N), so its size is $M \times N$. The size of matrix U has $M \times M$ and that of matrix S is $M \times N$. The matrix V is consisted of the size of $N \times N$.

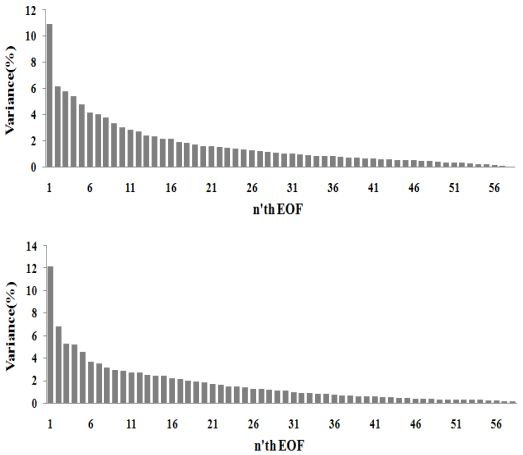

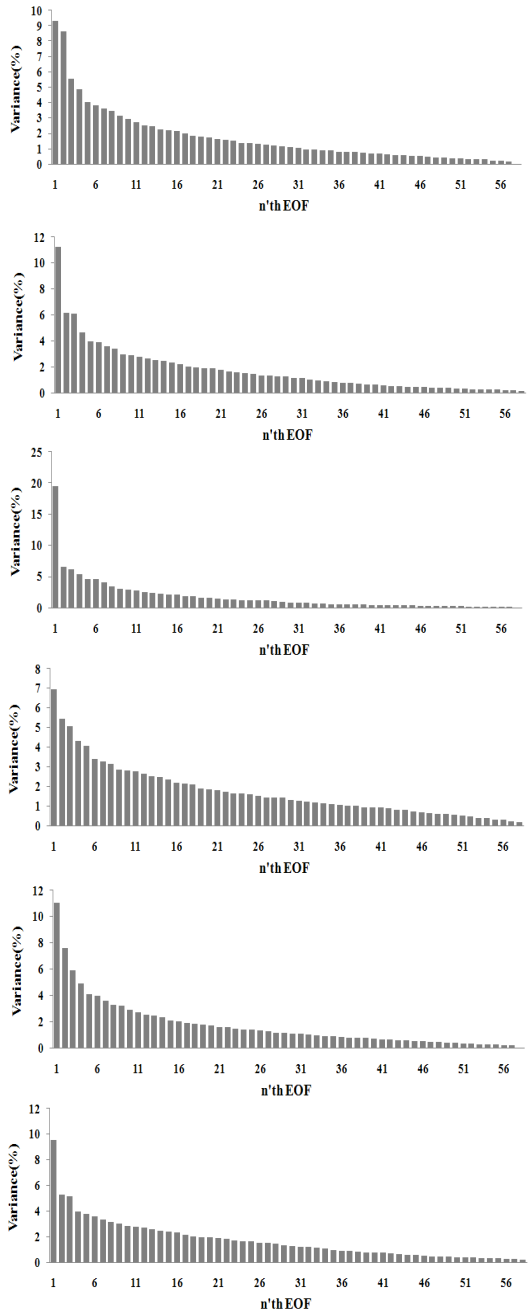

Fig. 9. Variance of EOF (Left side : KMA RCM, Right side : CNCM3) – from top to down is Case 1 to Case 4

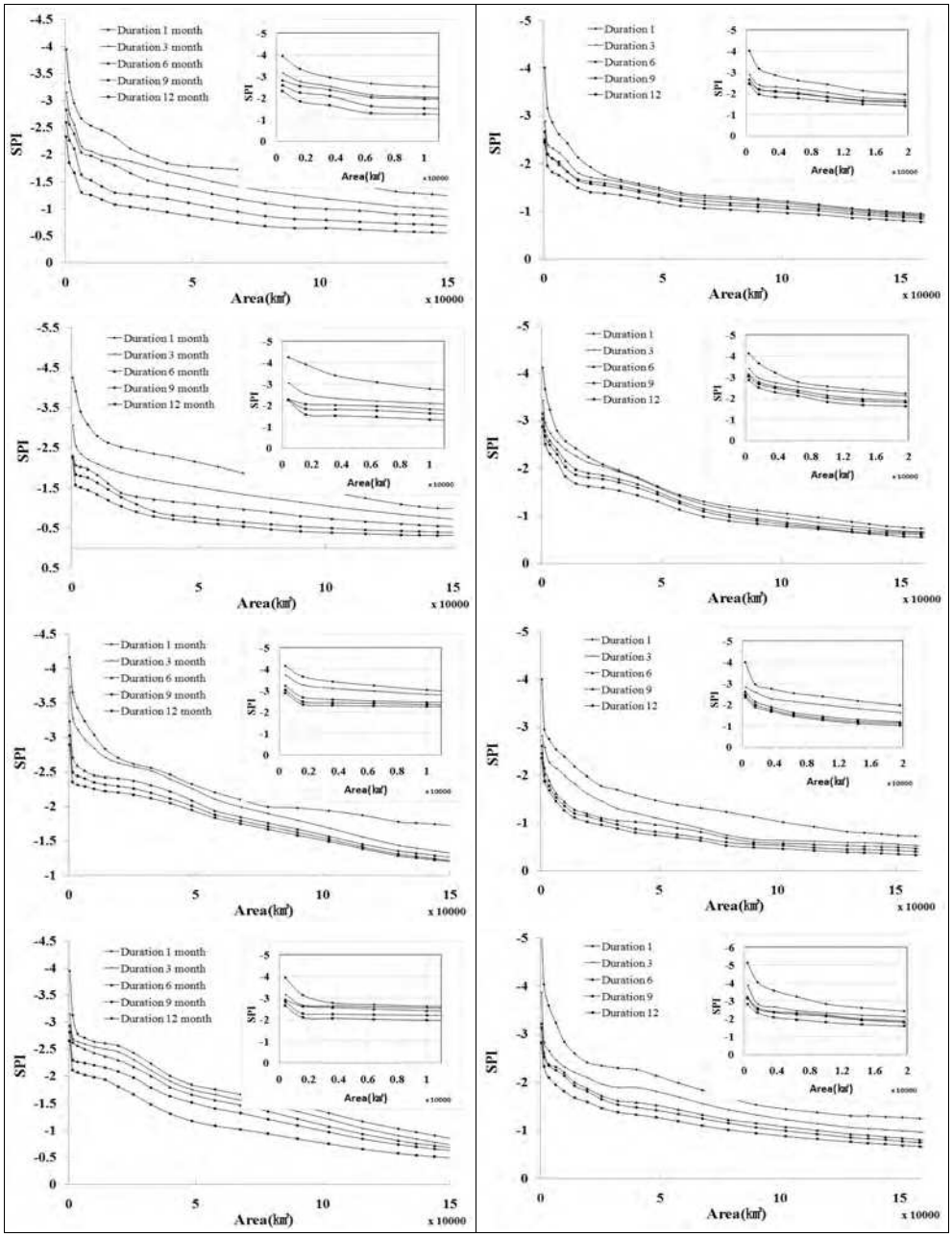

Fig. 10. SAD curves for whole South Korea (Left side : KMA RCM, Right side : CNCM3) – from top to down is Case 1 to Case 4

The number of EOF is as many as 58, which is the same number with the stations used. In this study, every variance value from each CASE was arranged by all models presented here. Those variance values were marked as the percentages(%) of the total variance values to present the variance values of each EOF.
As for KMA RCM, it was expected that two strong spatial patterns would appear in CASE2 followed by one pattern of spatial variability with a strong explanatory power in CASE3. Then, CASE4 showed various types of partial variability. In contrast, the CNCM3 model maintained the pattern of spatial variability with an apparent explanatory power from CASE1 to CASE2 but overall, the spatial variability pattern did not seem to be significantly different in CASE3. However, the variances of the first EOF are expected to show apparently different characteristic.
In order to draw the SAD curve, it is necessary to expand spatially each EOF. For the spatial expansion of each EOF, the kriging method can be used. The whole Korea is divided into 10,000 (100×100) grids with a width and length of six kilometers. Hisdal and Tallaksen (2003) also applied the kriging method to assign an EOF's value at each grid point. Such spatially expanded EOFs are then inversely transformed to calculate SPI time series at each grid point. Finally, averaging spatially and temporally, one can calculate the maximum spatio-temporally averaged SPI value at a specified temporal and spatial scale to draw SAD curve. Figure 10 shows drought severity-affected area curves for the duration of 1, 3, 6, 9 and 12 months.
SAD curve serves as an indicator showing how drought severity, which is estimated by using SPI to assess the drought prone area, changes by area and duration. As a result of generating the SAD curve for each model, it was predicted that the smaller the affected area is, the higher the severity is likely to be in CASE2 representing the near future while except for the drought with the three month duration, behaviors similar to CASE1 were seen in CASE3. Since overall drought severity in CASE4 became higher, drought is expected to cause the most severe damage.

5. Summary and conclusions

In this study, the impact of climate change on drought in Korea was evaluated. In order to consider such climate change impact, French GCM, CNCM3 and RCM by National Institute of Meteorological Research (NIMR) under the Korea Meteorological Administration were used. In addition, downscaled monthly precipitation was estimated by using SK-NN, and NIMR's RCM was used to calculate SPI for 58 stations in Korea. The SPI was used to compare the number of drought occurrences and average severity of the total drought, and droughts both with the duration of over six months and over twelve months. Drought severity by spatial extent in accordance with duration was calculated, generating SAD curve by utilizing SPI. The analysis of this study shows that the risk of drought in Korea is growing. Therefore, it is important to come up with responsive measures for drought from a mid-and-long term perspective.

6. Acknowledgement

This work was supported by the National Research Foundation Grant funded by the Korean Government (MEST) (**NRF-2009-220-D00104**)."

7. References

Andreadis, K. M., Clark, E. A., Wood, A. W., Hamlet, A. F., Lettenmaier, D. P. (2005) Twentieth-Century Drought in the Conterminous United States. Journal of Hydrometeorology Vol. 6, No. 6, pp. 985-1001

Benjamin, L. H. (2002) The Long-Range Predictability of European Drought. Degree of doctor of philosophy. University college London.

Buishand, T. A., Brandsma, T. (2001) Multisite simulation of daily precipitation and temperature in the Rhine Basin by nearestneighbor resampling, Water Resources Research, Vol. 37, No. 11, pp. 2761–2776

Casdagli, M. (1992) Chaos and deterministic versus stochastic nonlinear modeling, Journal of the Royal Statistical society, Statistics in society, Series B 54, pp. 303–324

Casdagli, M. and Weigend, A. (1994) Exploring the Continuum Between Deterministic and Stochastic Modelling, Forecasting the Future and Understanding the Past, Eds. A. S. Weigned and N. A. Gershenfeld, SFI Studies in the Sciences of Complexity, Proc. Vol. XV, Addison-Wesley, 993

Dubrovsky M., Buchtele, J., Zalud, Z. (2004) High-frequency and lowfrequency variability in stochastic daily weather generator and its effect on agricultural and hydrologic modelling, Climatic Change, Vol. 63, pp. 145–179

Durman, C.. F., Gregory, J. M., Hassell, D. C., Jones, R. G. and Murphy, J. M. (2001) A comparison of extreme European daily precipitation simulated by a global and a regional climate model for present and future climates. Quarterly Journal of the Royal Meteorological Society, Royal Meteorological Society, Vol. 127, No. 573, pp. 1005-1015

Fowler, H. J., Kilsby, C. G. and Stunell, J. (2007b) Modeling the impacts of projected future climate change on water resources in north-west England. Hydrologic & Earth System Sciences, EGU, Vol. 11, No. 3, pp. 1115-1126

Hamlet, A.F., Lettenmaier, D.P. and Snover, A. (2003) Climate change streamflow scenarios for critical period water planning studies:A technical methodology. Journal of Water Resources Planning and Management, ASCE, in review

Hashino, T., Bradley, A. A., and Schwartz, S. S. (2007) Evaluation of bias-correction methods for ensemble streamflow volume forecasts. Hydrology and Earth System Science, EGU, Vol. 11, pp. 939-950

Henriques AG, Santos MJJ. 1999. Regional Drought Distribution Model. Phys. Chem. Earth (B), Vol. 24, No. 1-2, pp. 19–22

Hisdal, H., Tallaksen, L. M. (2003) Estimation of regional meteorological and hydrological drought characteristics : a case study for Denmark. Journal of Hydrology, Vol. 281, No. 3, pp. 230-247

Kim T. W., Valdés J. B., Aparicio J. (2002) Frequency and Spatial Characteristics of Droughts in the Conchos River Basin, Mexico. Water International, Vol. 27, No. 3

Kim B. S., Kim B. K., Kyoung M. S., Kim H. S. (2008) Impact Assessment of Climate Change on Extreme Rainfall and I-D-F Analysis. Journal of Korea Water Resources Association. Korea Water Resources Association. Vol. 41, No. 4, pp. 379-394

Kyoung M. S., Lee Y. W., Kim H. S., Kim B. S., (2009a) Assessment of Climate Chanage Effect on Temperature and Drought in Seoul : Based on the AR4 SRES A2 Senario. Korean Society of Civil Engineers Journal of Civil Engineering. Korean Society of Civil Engineers. Vol. 29, No. 2B, pp. 267-276

Kyoung M. S., Lee J. K., Kim H. S. (2009b) Downscaling Technique of Monthly GCM Using Daily Precipitation Generator. Korean Society of Civil Engineers Journal of Civil Engineering. Korean Society of Civil Engineers. Vol. 29, No. 5B, pp. 441-452

Kyoung M. S. (2010) Assessment of Climate Change Effect on Drought and Frequency Based Precipitation, Department of Civil Engineering, INHA University, Incheon, Korea. pp. 44-48

Lall, U., Rajagopalan, B., Torboton, D. G. (1996) A nonparametric wet/dry spell model for resampling daily precipitation, Water Resources Research, Vol. 32, No. 9, pp. 2803–2823

Lall, U., Sharma, A. (1996), A nearest neighbour bootstrap for time series resampling, Water Resources Research, Vol. 32, No. 3, pp. 679–693

Matheron G. 1963. Principles of Geostatistics. Econom. Geol., Vol. 58, No. 8, pp. 1246–1266

McKee, T. B., Doesken, N. J. and Kleist, J. (1993) The relationship of drought frequency and duration to time scales. Preprints, 8th Conference on Applied Climatology, 17-22 January, Anaheim, California, pp.179-184.

Mishra AK, Singh VP. 2009. Analysis of drought severity-area-frequency curves using a general circulation model and scenario uncertainty, J. Geophys. Res., Vol. 114

Palmer, R., Wiley, M., Kameenui, A. (2004) Will Climate Change Impact Water Supply and Demand In the Puget Sound?, Department of Civil and Environmental Engineering University of Washington, Seattle WA.

Panofsy, H. A., Brire, G. W. (1963) Some application of Statistics to Meteorology, Pennsylvania State University, University Park, Pennsylvania, pp. 224.

Perry and Niemann, (2008) Generation of soil moisture patterns at the catchment scale by EOF interpolation. *Hydrol. Earth Syst. Sci.* 12: 39–53.

Rajagopalan, B., Lall, U., (1999) A k-nearest neighbour simulator for daily precipitation and other variables, Water Resources Research, Vol. 35, No. 10, pp. 3089–3101

Sauquet E, Krasovskaia I, Leblois E. (2000) Mapping mean monthly runoff pattern using EOF analysis. *Hydrology and Earth System Sciences* 4(1): 79-93.

Sharif, M., Burn, D. H. (2006) Simulating climate change scenarios using improved K-nearest neighbor model, Journal of Hydrology, Vol. 325, pp. 179-196

Viron O, Panet I, Diamaent M. (2006) Extracting low frequency climate signal from GRACE data. *eEarth* 1: 9-14.

Wood, A. W., Leung, L. R., Sridhar. V. and Lettenmaier, D. P. (2004) Hydrologic implications of dynamical and statistical approaches to downscaling climate model outputs. Climatic Change, Vol. 62, Issue 1-3, pp. 189-216.

Yates, D., Gangopadhyay, S., Rajagopalan, B., Strzepek, K. (2003) A technique for generating regional climate scenarios using a nearest-neighbor algorithm, Water Resources Research, Vol. 39, No. 7, pp. 7-14

Young, K.C., (1994) A multivariate chain model for simulating climatic parameters with daily data, Journal of Applied Meteorology, vol. 33, pp. 661–671

Yoo CS, Kim SD. (2004) EOF Analysis of surface soil moisture field variability. *Advance in Water Resources* 27(8): 831-842, DOI: 10.1016.

Zveryaev II, Arkhipkin AV. (2008) Structure of climate variability of the Mediterranean sea surface temperature. Part II. Principle modes of variability. *Russian Meteorology and Hydrology* 33(7): 446–452, DOI: 10.3103/S1068373908070066.

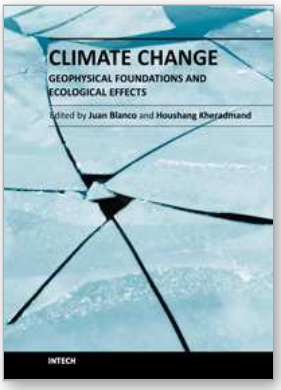

Climate Change - Geophysical Foundations and Ecological Effects

Edited by Dr Juan Blanco

ISBN 978-953-307-419-1
Hard cover, 520 pages
Publisher InTech
Published online 12, September, 2011
Published in print edition September, 2011

This book offers an interdisciplinary view of the biophysical issues related to climate change. Climate change is a phenomenon by which the long-term averages of weather events (i.e. temperature, precipitation, wind speed, etc.) that define the climate of a region are not constant but change over time. There have been a series of past periods of climatic change, registered in historical or paleoecological records. In the first section of this book, a series of state-of-the-art research projects explore the biophysical causes for climate change and the techniques currently being used and developed for its detection in several regions of the world. The second section of the book explores the effects that have been reported already on the flora and fauna in different ecosystems around the globe. Among them, the ecosystems and landscapes in arctic and alpine regions are expected to be among the most affected by the change in climate, as they will suffer the more intense changes. The final section of this book explores in detail those issues.

InTech Europe
University Campus STeP Ri
Slavka Krautzeka 83/A
51000 Rijeka, Croatia
Phone: +385 (51) 770 447
Fax: +385 (51) 686 166
www.intechopen.com

InTech China
Unit 405, Office Block, Hotel Equatorial Shanghai
No.65, Yan An Road (West), Shanghai, 200040, China
中国上海市延安西路65号上海国际贵都大饭店办公楼405单元
Phone: +86-21-62489820
Fax: +86-21-62489821